The Variable-delay Polarization Modulator

M. Krejny[a], D. T. Chuss[b], G. Novak[a], G. M. Voellmer[b], E. J. Wollack[b], C. K. Walker[c], M. Jackson[b], D. J. Benford[b], J. G. Staguhn[b], S. H. Moseley, Jr.[b], C. Kulesa[c], C. Y. Drouet d'Aubigny[c], D. R. Golish[c], R. F. Loewenstein[d]

[a]Northwestern Univ., 2131 Tech Dr., Evanston, IL 60208, USA;
[b]NASA Goddard Space Flight Ctr., Greenbelt, MD 20771, USA;
[c]The Univ. of Arizona/Steward Observatory, Tucson, AZ 85721, USA;
[d]Yerkes Observatory, University of Chicago, Williams Bay, WI 53191 USA

ABSTRACT

Precise astronomical polarization measurements generally require the use of polarization modulation. We have developed a new modulator, the Variable-delay Polarization Modulator (VPM) which uses two modified Martin-Puplett interferometers to induce a physical path length difference between polarization components. This highly durable and efficient device can easily be adapted to a wide range of wavelengths and temperatures, making it well suited for air- and space-borne facilities. This paper discusses the basic modulator design and a comparison to the half-wave plate, as well as details of VPM tests conducted at the Submillimeter Telescope Observatory (SMTO).

Keywords: polarimetry, instrumentation, far-infrared, sub-millimeter

1. INTRODUCTION

Polarization from the far-infrared through millimeter wavelengths provides insight into the roles of magnetic fields in star formation as well as the early universe. Polarization modulation is a technique used to distinguish between the polarization of the astrophysical source and extraneous polarization due to the instrument itself.

A new type of modulator, the Variable-delay Polarization Modulator (VPM), has significant advantages over the half-wave plate (HWP) technology that is currently in widespread use. Using two sets of mirrors and polarizing grids, the incoming polarization can be "rotated" by small linear motions via piezoelectric motors. In contrast, HWPs must be turned repeatedly through large angles, leading to the possibility of mechanical failure due to frictional wear. In addition, VPMs are easily tunable over a wide range of wavelengths and have no dielectric loss. These devices, or variations thereof, may find use in various far-infrared through millimeter polarimeters.

In this paper we review the basic theory behind the VPM, and compare it to the HWP modulator design. Also, we present preliminary results from the first engineering run of Hertz/VPM, an experiment designed to test these new modulators. This experiment runs at the U. of Arizona's SMTO telescope on Mt. Graham, and makes use of the Hertz polarimeter formerly operated at the Caltech Submillimeter Observatory.[1] Finally, we present an example application for these multi-wavelength devices.

2. STOKES PARAMETERS AND POLARIZED LIGHT

Stokes parameters are one way to completely characterize the polarization state of a light wave. The four Stokes parameters, I, Q, U, and V describe the total intensity, linear polarization, and circular polarization of the wave. For linearly polarized light, Q measures the preponderance of horizontal (0°) over vertical (90°) polarization, while U is the preponderance of 45° over 135° polarization. V is the preponderance of left circularly polarized light (LCP) over right circularly polarized light (RCP). Stokes space can be visualized through the use of the Poincare sphere (see Figure 1). The polarization states Q, U, and V are set along the axes, and any point in or on the sphere is a combination of these three states. Linear polarization lies completely within the QU plane, while circular polarization lies on the V axis.

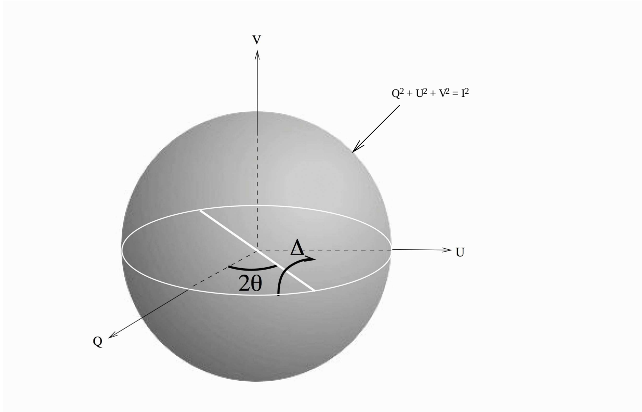

Figure 1. The Poincare Sphere. The surface denotes completely polarized light, while points within the sphere signify partially polarized light. HWP rotations of θ correspond to rotations in the QU (linear polarization) plane of 2θ; the VPM can also rotate a point out of the plane into circular or elliptical polarization states (Δ).

Any point lying on the surface of the sphere denotes completely polarized light, and in this case the intensities of the Stokes parameters add in quadrature to give the total intensity:

$$Q^2 + U^2 + V^2 = I^2. \tag{1}$$

However, if the point does not lie on the surface of the sphere (partially polarized light), the Stokes parameters add up to:

$$Q^2 + U^2 + V^2 = (PI)^2, \tag{2}$$

where P denotes the percentage of polarized light.[2] Stokes parameters are useful in that they allow simple addition of multiple partially polarized light sources. For incoherent sources, Stokes parameters add linearly.

3. NEED FOR POLARIZATION MODULATION

Ground-based FIR and submillimeter polarimetry involves the difficult task of measuring polarized signals that are on the order of 10^{-2} of the source flux and 10^{-6} of the sky background. The desire to maximize the signal-to-noise ratio requires us to minimize outside flux sources and increase observable source flux as much as possible. In addition to atmospheric flux, optical components such as windows, lenses, and filters, can cause spurious polarization. The use of a modulator helps separate source polarization from these extraneous effects.

To view the polarization of an object, a polarizing grid is used to break the incoming light into two orthogonal polarization components: reflected (R) and transmitted (T) light. In some instruments, only one component of the light is observed,[3] while other polarimeters detect both components simultaneously using two separate arrays. The Hertz polarimeter utilizes two separate arrays,[1] so we shall discuss the latter method. For each modulation position, the polarization signal S_{mod} is defined as:[4]

$$S_{mod} = (R_{mod} - fT_{mod})/(R_{mod} + fT_{mod}), \tag{3}$$

where f is the relative gain of the two arrays, and R_{mod} (T_{mod}) is the strength of the R (T) component measured at a single modulator position. By recording a single value of S_{mod} for each of N modulator positions we obtain one polarization "cycle". By fitting a sine curve to S_{mod} we determine the polarization degree and polarization angle from the amplitude and phase of the sine curve, respectively. The simplest way to modulate the source is to wait for the object to rotate in the sky, or to rotate the telescope with respect to the object. To obtain data in a timely manner, however, we look to other methods. We discuss two polarization modulators, the HWP and the new modulator which we have constructed and tested, the variable-delay polarization modulator (VPM).

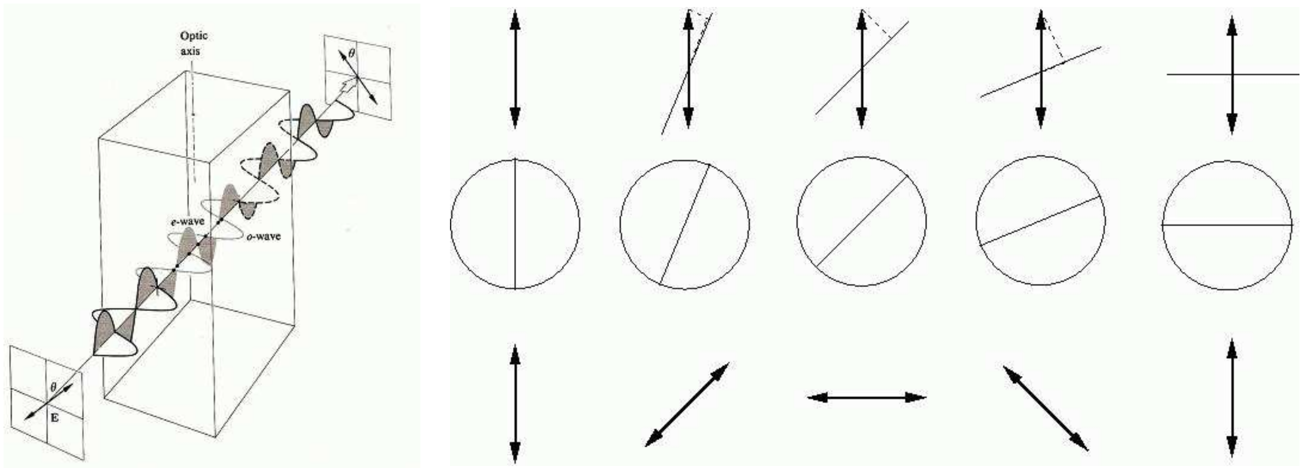

Figure 2. Left: A HWP introduces a phase delay of $\lambda/2$ between orthogonal polarization components.[5] Right: As a HWP is rotated by an angle θ, the outgoing polarization is rotated by an angle 2θ.

4. THE HALF-WAVE PLATE

Traditionally, a HWP is most commonly used to modulate linear polarization. Its birefringent material delays one component of polarization by exactly one half wavelength with respect to the other (see Fig. 2). If the HWP is rotated by an angle θ the outgoing polarization vector is rotated by 2θ. On the Poincare sphere, these rotations take place in the QU plane (Fig. 1).

Despite the simplicity of its design and the ubiquitousness of its use, the HWP has many disadvantages. First, rotational motion can cause excessive stress to the bearings and components involved. A lifetime on the scale of only a few years is common for many HWPs, which is acceptable for ground-based instruments, where servicing is relatively easy. For an air-, balloon-, or space-based instrument (or for instruments operated at remote locations like the South Pole), components with longer lifetimes are highly desirable. Also, the thickness of the material allows a HWP to be used only for one waveband. An achromatic design[3] stacks multiple layers together to create a large-bandwidth HWP, but the use of multiple HWPs can increase signal loss and makes the HWP more difficult to treat with commonly used anti-reflection coating.

5. THE VARIABLE-DELAY POLARIZATION MODULATOR

We have designed a new modulator consisting of dual modified Martin-Puplett Interferometers (MPIs). An MPI allows the user to modulate the polarization using linear translation (via piezoelectric motors) instead of rotation. The amount of motion involved is very small, allowing for equipment with long lifetimes.

This architecture has several other advantages over a HWP. First, the use of reflective elements eliminates the need for lossy dielectrics that must be antireflection coated and often cooled for the best possible efficiencies. Also, assuming the grids are perfect over a large range of wavelengths, the wavelength scale is set only by the grid-mirror distance. Therefore, tuning to multiple frequencies is trivial. For any given wavelength, the MPI and HWP have similar effective polarization modulation bandwidths.[2] This tunable grid-mirror distance also allows measurement of circular polarization.

We now discuss the main ideas behind the dual-MPI design. As evident from the design of the HWP, we see that the main ingredient in changing the polarization state is to introduce some optical path length difference between two orthogonal components of linear polarization. One method for doing this is to place a polarizing grid in front of a mirror. Light at near-normal incidence upon the grid is separated into orthogonal polarizations, one reflected and one transmitted through to the mirror. After the latter light beam is reflected and passes back through the grid, it has passed through a path length difference of l. For a grid-mirror separation distance d and angle of incidence θ_{inc}, the total pathlength distance is:

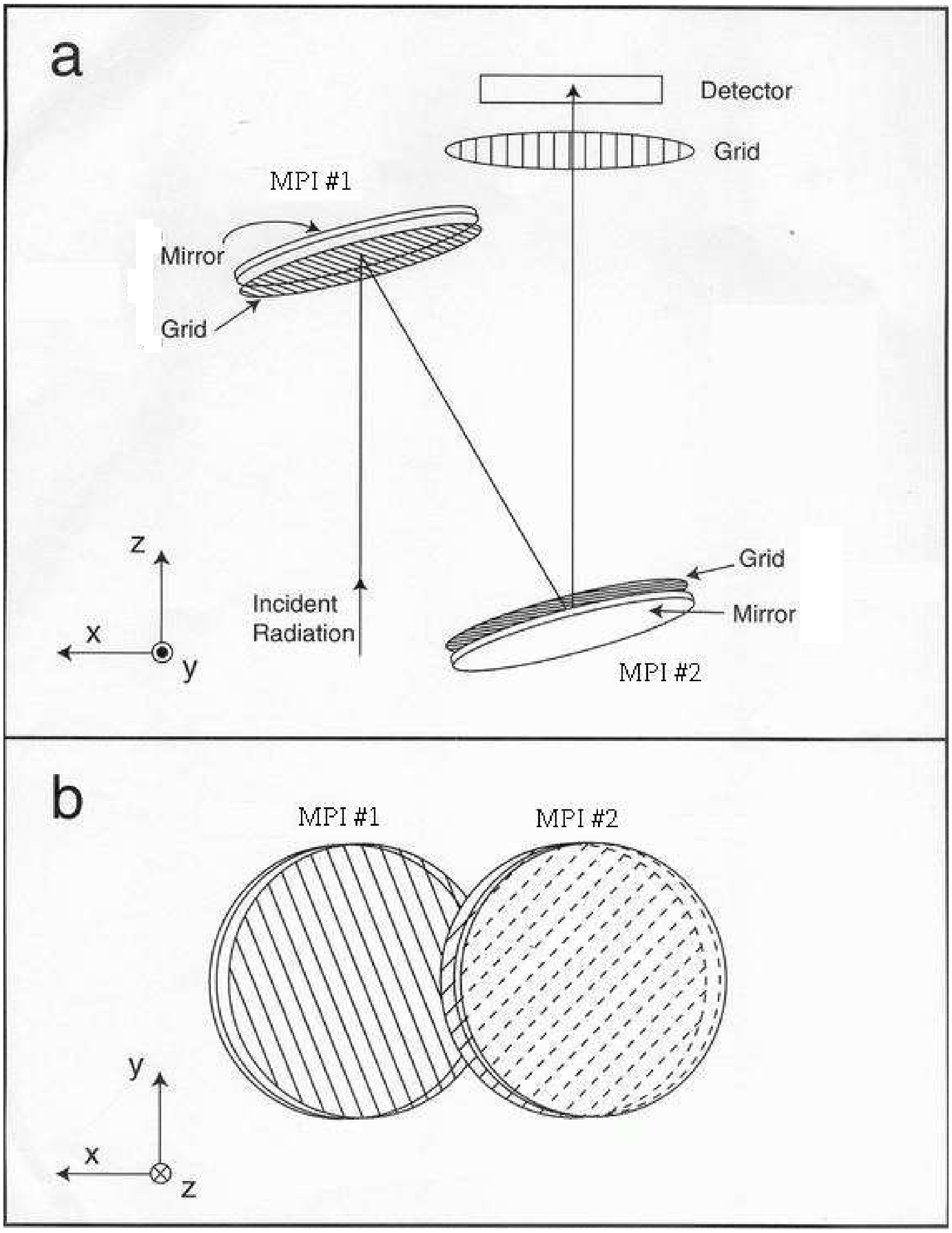

Figure 3. Two views (see axes at bottom left of each view) of the basic VPM optics setup. The use of two Martin-Puplett Interferometers (MPIs) allows modulation over all Stokes space. Grid orientations of the two MPIs are rotated 22.5° with respect to each other.

$$l = \frac{d}{\cos\theta_{inc}}(1 + \cos 2\theta_{inc}) \tag{4}$$

We then set this path length to equal either a full or half wavelength.

By switching the mirror-grid separation between a half-wave and full-wave delay, the MPI acts similarly to a HWP being turned "on" and "off". However, this is not sufficient to modulate any arbitrary direction of linear polarization. Incoming polarized light with polarization either completely parallel or completely orthogonal to

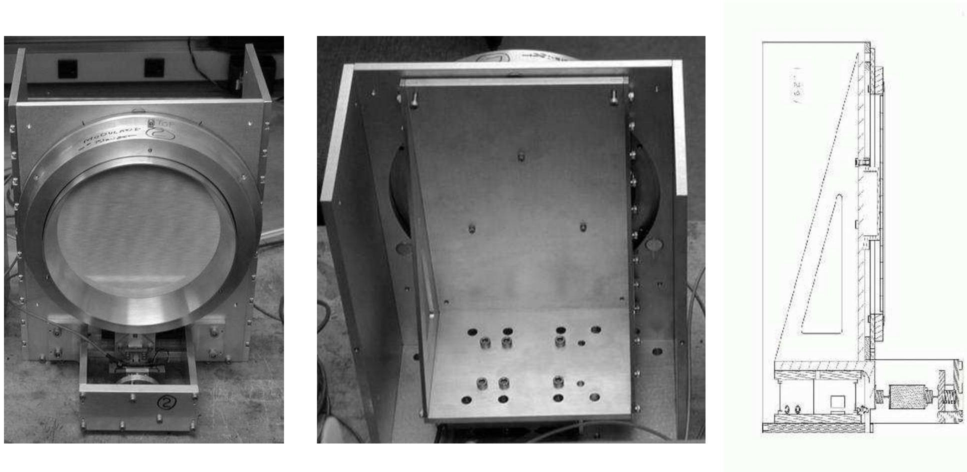

Figure 4. Views of one MPI. Left: front view showing piezoelectric motor, grid support, and grid straightener. Middle: back view showing mirror support. Double-blade flexure underneath. Right: side view diagram. (Note: grid staightener not shown in this view.)

the polarization axis of the HWP (or, equivalently, to the axis of the grid) will experience no change. Therefore, one MPI is not sufficient.

Accordingly, we incorporate a second MPI, with the grids rotated 22.5° with respect to those of the first set. Any light not modulated by the first MPI will be modulated by the second set.[2] Figure 3 shows the basic dual-MPI configuration. We refer to this design for a modulator as a Variable-delay Polarization Modulator, or VPM.

For our purposes, we have only described modulation of linearly polarized signals. However, by setting l to $\lambda/4$ or $3\lambda/4$, one can also observe circularly polarized light. On the Poincare sphere, the VPM can rotate both in the QU plane and out of it, as denoted by Δ. This is shown in Figure 1.

6. THE HERTZ/VPM EXPERIMENT

6.1. The Goddard VPMs

Each MPI consists of a mirror and wire grid. The grid is supported on the outer aluminum casing and is attached to the casing with rare earth magnets. Set screws are used to control the distance between the grid and the casing, which in effect controls the parallelism of the grid-mirror system.

The mirror is connected to the casing and supported by a double-blade flexure linear bearing.[6] This bearing was designed by G. Voellmer at NASA/GSFC to enable parallel translation of the mirror.

Attached to the front of the aluminum casing is the piezoelectric motor. Also attached to the front of the casing is a grid flattener that rests on the polarizing grid and increases the flatness of the grid. Figure 4 shows one MPI from various angles.

6.2. The Heinrich Hertz Telescope

The Heinrich Hertz Telescope (HHT) is a 10m telescope operating at submillimeter/millimeter wavelengths (λ = 0.3-2mm). It is located at the Submillimeter Telescope Observatory (SMTO) on Mt. Graham, Arizona. Submillimeter astronomy is best carried out during the months from November to April, when the 225 GHz opacity is less than 0.06, about 20% of the time. For 350 μm, this corresponds to a zenith transmission of roughly 25% or better.

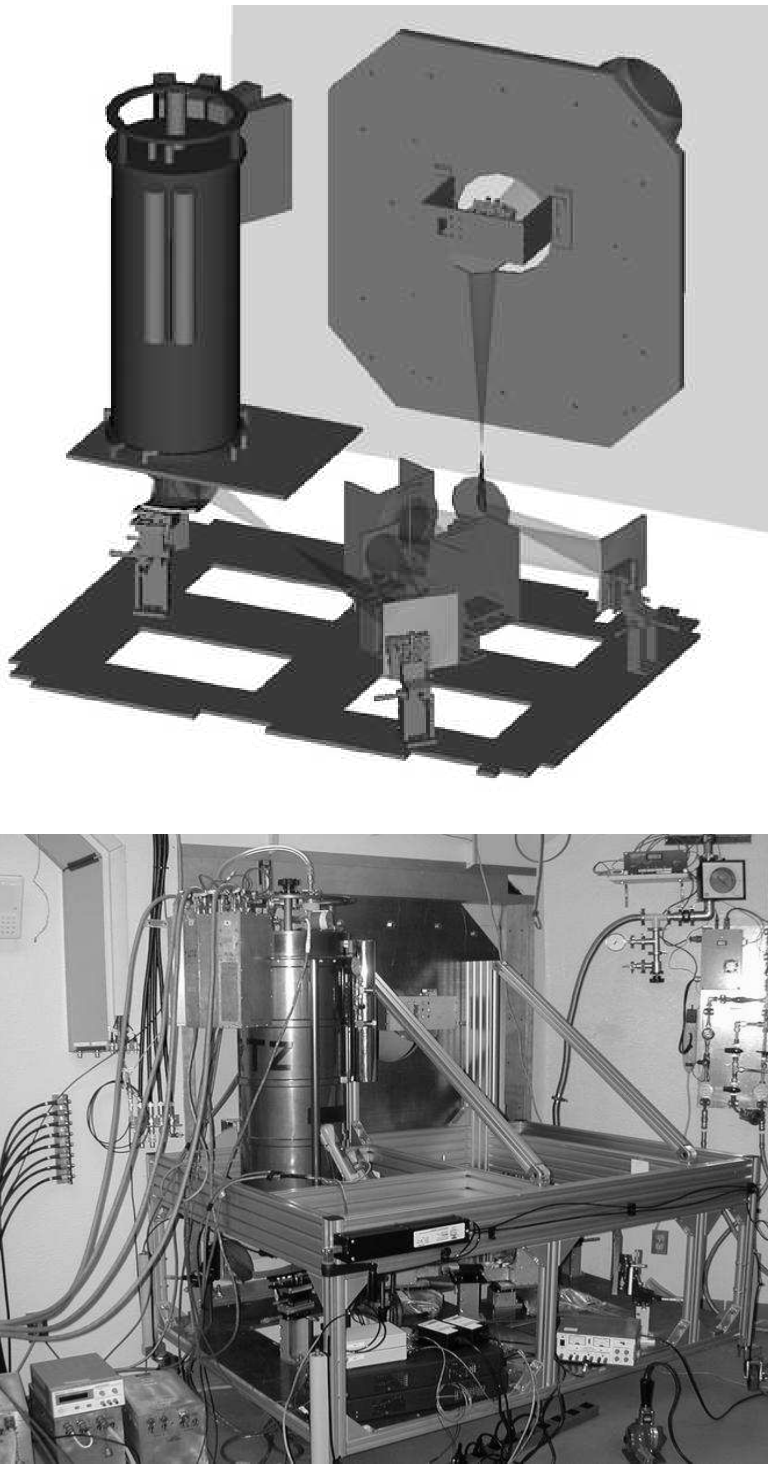

Figure 5. Top: Optics design for Hertz polarimeter with VPM. Beam is bent down from telescope mount, then collimated for passage through VPM. The beam is then refocused and sent up into Hertz. Bottom: Experiment on the HHT.

6.3. The Hertz Polarimeter

Hertz is a 350 μm polarimeter developed at U. Chicago and previously operated at the Caltech Submillimeter Observatory (CSO).[1] It contains two 32-pixel Helium-3 cooled bolometer arrays which measure orthogonal polarization components simultaneously. Hertz also includes a cooled HWP located at a pupil stop.

6.4. Optics

Hertz was designed to accept an image of the primary (ip) at the pressure window. A second ip is formed inside Hertz, and the HWP is located within 4 cm of this second ip. A wire grid is located farther down the optical path. The pixel separation is $18''$.[7]

Figure 5 (top image) shows the full Hertz/VPM optics design. The experiment is mounted at a Nasmyth focus. The first (flat) mirror bends light down into the optics plane. The beam is collimated before passing through the VPM, then refocused up into the polarimeter. At bottom of Figure 5 we show a photo of the experiment.

6.5. Modulator Control

At the CSO, the Hertz HWP was controlled through a custom-built computer. For operation at U. of Arizona, we decided to use a commercially available computer designed for instrument control: the Ethernet Data Acquisition System, or EDAS. Its modular system allows us to control hardware through several different types of interfaces. For the HWP, commands and position readings were accomplished through analog I/O. The VPM piezoelectric motors require serial communication with a servo controller.

The EDAS uses flash RAM in place of a hard disk, so it is less likely to fail than a conventional computer. Also, communication with the EDAS is via the internet, so devices can be easily controlled remotely.

6.6. Data Acquisition

To effectively remove background and noise sources at these wavelengths, special observation techniques are used.[4] Background removal is accomplished first by "chopping," or quickly moving the secondary mirror back and forth. This frequency must be fast enough so that $1/f$ noise from the atmosphere is not dominant (frequency ranges from 3-15 Hz). One can relate the motion of this mirror to the telescope switching between two beams on the sky, a left and a right. The object to be observed is placed in one beam ("on-source") while the other beam looks at blank sky ("off-source"). The computer then reads a (demodulated) signal consisting of the flux from the left beam minus the flux from the right.

The output of the bolometer array is analog voltages. These voltages are multiplied by pre-amplifiers and then sent to our data acquisition box, which converts the voltages to a digital signal. From there, the digital output is sent to a Macintosh data acquisition computer. The computer includes a Digital Signal Processing (DSP) card developed at NASA/GSFC that interfaces with a Macintosh NuBus and with the data acquisition box.

Our data acquisition software was developed specifically for far-IR/submillimeter astronomy. This work was done at the U. of Chicago where Hertz was developed. During our engineering run with Hertz/VPM in April 2006, data were taken in two different modes: the first consisted of fixed modulator positions and a rotating HWP (i.e., a "HWP file"), and the other kept the HWP position fixed and moved the VPM ("VPM file"). Six modulator positions were used for each such polarization cycle.

7. PRELIMINARY RESULTS

7.1. Parallelism of VPM

The VPM appears to be fairly robust. The mirror-grid parallelism was achieved by three-point alignments under a microscope; the surfaces were found to be parallel to within $5\,\mu$m. The double-blade flexure bearings maintained a parallelism of $1.5\,\mu$m under full throw.[6] Finally, coupling to the secondary chopping mirror created an error in modulator position, minimized with a chopping frequency of 2.9 Hz, of roughly $\pm\ 2\,\mu$m.

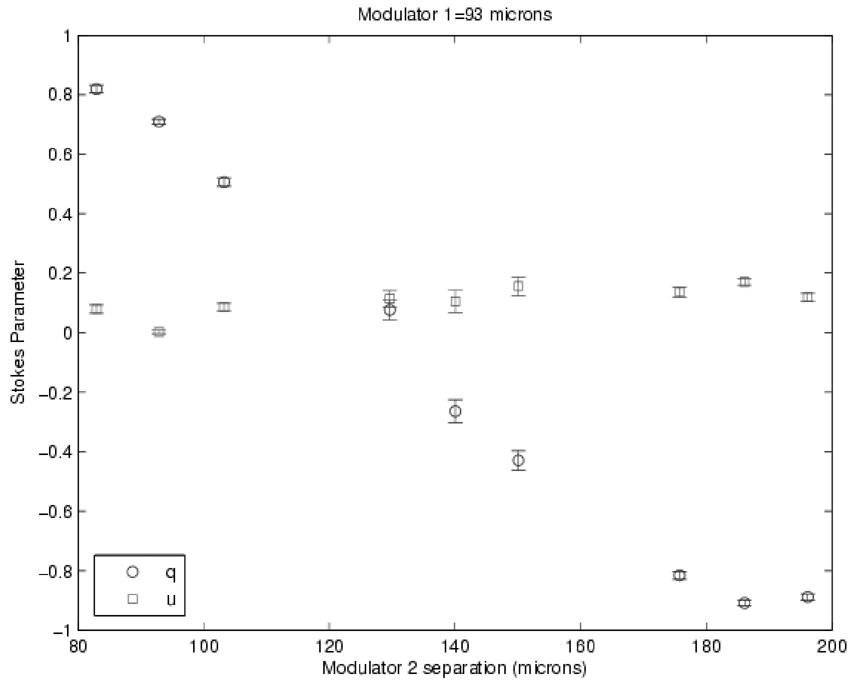

Figure 6. The plot shows the normalized Stokes parameters q and u as a function of the delay introduced by the second modulator. The first modulator is held fixed at a half-wave delay. See section 7.2 for further discussion.

7.2. Polarimetry

For most nights, high atmospheric opacity limited the objects viewed to bright planets including Jupiter and Saturn. Objects were observed both with and without a polarizing grid placed in the beam. Low opacity on the last night allowed us to take polarimetry data for SgrB2, DR 21, and G34.3. These data were collected without a polarizing grid in the beam.

Figure 6 shows polarization data for Saturn, with a polarizing grid in the beam. The grid was orientated perpendicular to the grid of the second modulator (the second modulator is rotated 45° with respect to the grid in Hertz, hence the grid transmits light in a U polarization state). Thus, the second modulator cannot modulate the incoming polarized light unless its polarization state is changed by the first modulator. The figure shows the values of normalized q and u measured by Hertz as a function of the delay introduced by the second modulator, for the case where the delay introduced by the first modulator is one-half of a wave. The effect of the first modulator is to change the polarization state from U to Q, thus allowing the second MPI to modulate q between +1 and -1. Note that u is approximately zero, as expected. Signals were collected using several other modulation schemes, and we are currently analyzing these data.

8. FUTURE PLANS

8.1. New Measurements

In Fall 2006 we plan to operate the Hertz polarimeter with the VPM at least once more at the SMTO. During that time we will acquire more polarimetry data, taking advantage of the best 350 μm weather by using priority scheduling.

A full analysis of the current (and future) data will include an accurate measure of the instrumental polarization introduced by the optics system. In the upcoming year we plan to observe more calibrated sources under a range of high and low sky noise conditions.

8.2. Scientific Application: T Tauri Star Disks

Observations suggest that dust grains in T Tauri star (TTS) disks are coagulating, forming particles as big as ~ 1 mm or even larger.[8–10] Thus, by observing these disks we might be able to study the first steps in planet formation. Because particles cannot efficiently scatter light for wavelengths much bigger than the particle size, and because scattered light is usually polarized, polarimetry can provide a probe of grain size. Here we describe a program of multi-wavelength polarimetery that we are proposing to carry out at the Submillimeter Array (SMA), the Caltech Submillimeter Observatory (CSO), and the Very Large Array (VLA). Our goal is to confirm and study grain-size growth in TTS disks.

In interstellar clouds, dust grains are much too small ($< 1\ \mu$m) to efficiently scatter submillimeter radiation; the submillimeter polarization measured in these clouds cannot be due to scattering and must instead be due to thermal emission by magnetically aligned grains.[11] However, when observers at the James Clerk Maxwell Telescope (JCMT) succeeded in detecting polarization of order several percent in the submillimeter emission from two approximately edge-on TTS disks,[12] they may have become the first astronomers to detect polarized scattered light in the submillimeter. Although they in fact did not consider the possibility that their measurements could be due to scattering and instead attributed their results to thermal emission from aligned grains,[12] we will show that scattering is a plausible explanation for their measurements.

We calculate that if a substantial fraction of the grains have sizes of at least $30\,\mu$m, then for typical TTS disk parameters the submillimeter scattering optical depths will be non-negligible. Before describing these calculations, we note that the angles of polarization measured at JCMT[12] are perpendicular to the projected long axes of the disks, for both of their targets. This is consistent with the scattering hypothesis, because for a given scatterer there is more submillimeter radiation incident from a direction parallel to the plane than from a direction perpendicular to the plane. (As explained below, for very optically thick disks, the situation is more complicated.)

We have developed a toy model to explore the wavelength dependence of the polarization of submillimeter and millimeter radiation from an edge-on TTS disk. Our model is based on the assumption that the polarization can be estimated by first answering the following question: What fraction f of the thermal radiation from a "typical" grain is scattered at least once before escaping the disk? We then set the degree of observed polarization to $P = 0.3f$. We assume a uniform, cylindrical disk and estimate the scattered fraction as $f = (1 - exp(-\tau))$, where τ is the scattering optical depth computed for a line-of-sight passing through the disk and orthogonal to it.

The toy model described above overestimates P for disks that have high τ. This is because for high τ a typical scatterer "sees" a more nearly isotropic illumination, and thus the scattered radiation has little net polarization. Certainly the polarization is reduced to levels far below the toy model value $P = 0.3(1 - exp(-\tau))$. We simulate this effect by altering the P vs. τ curve as follows: For τ between zero and unity, we use the above formula, but as soon as τ increases above unity, we let P drop linearly, reaching zero for $\tau = 2$.

In our model the grains are of uniform size; we vary this size from $0.1\ \mu$m to 1 cm. Figure 7 shows that for a significant fraction of possible sizes we predict strong structure in the polarization spectrum. Such structure is the observational signpost of scattering, as polarization due to emission from sub-micron sized aligned grains should not have strong spectral dependence, although variations in P of up to a factor of 1.5 may be expected.[13] Of course, in real TTS disks not all grains are exactly the same size. Little is known about the distribution of grain sizes, but it seems unlikely that the very strong features seen in Figure 7 could be completely washed out by supposing a range of grain sizes. Probably some sizes will contribute more strongly to the emission, and the resultant polarization spectrum will still contain significant structure. We are currently developing a model that calculates P for a power-law grain size distribution.

To have the best chance of constraining grain size, we must observe the TTS disks across the full range of submillimeter and millimeter wavebands available. Currently, telescope time is needed at several different facilities to cover the full submm/mm wavebands available. A multi-wavelength camera, used in conjunction with the VPMs, would allow for more efficient data collection.

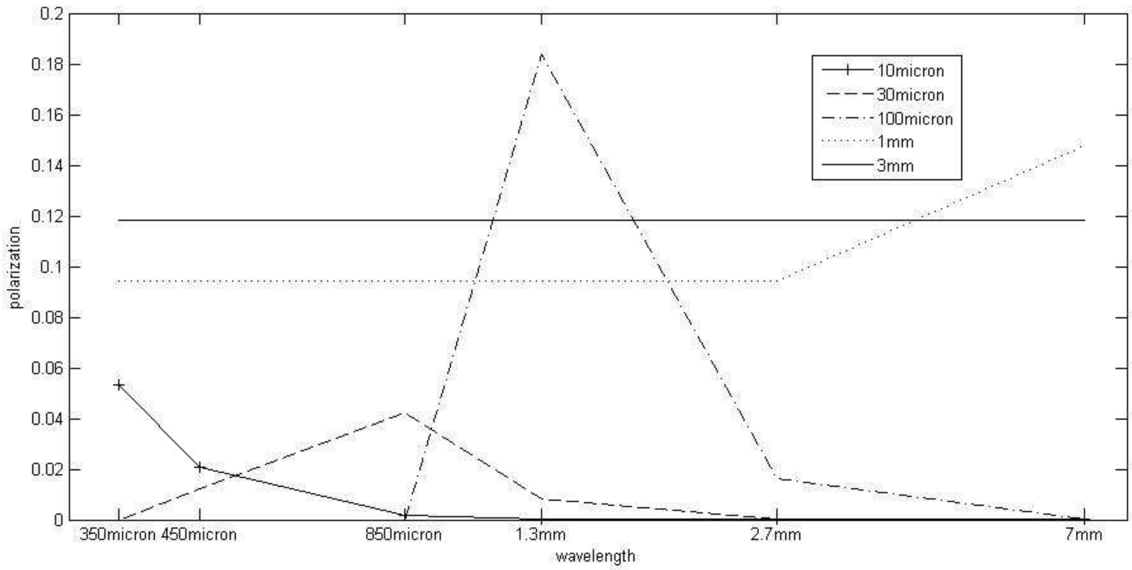

Figure 7. Toy model predictions for polarization by scattering, with disk diameter $D = 200$ AU, gas and dust disk mass $M = 0.1\ M_{\odot}$, and dust to gas mass ratio $A = 0.01$. Note that the assumed disk thickness does not affect the measured polarization for our model. Plots for different grain sizes shown. We obtain wavelength-dependent scattering cross-section data from a very simple grain model.[14] At $850\,\mu$m, a degree of polarization similar to that seen by Tamura et al. can be produced by grain sizes larger than $10\,\mu$m. Although 3 mm grains produce a flat polarization spectrum, the other grain sizes all show structure in their respective plots. Multi-wavelength observations could be more easily obtainable with a telescope outfitted with a VPM modulator.

REFERENCES

1. C. D. Dowell, R. H. Hildebrand, D. A. Schleuning, J. E. Vaillancourt, J. L. Dotson, G. Novak, T. Renbarger, and M. Houde, "Submillimeter Array Polarimetry with Hertz," *ApJ* **504**, p. 588, Sept. 1998.
2. D. T. Chuss, S. H. Moseley, G. Novak, and E. J. Wollack, "A Martin-Puplett architecture for polarization modulation and calibration," in *Ground-based Instrumentation for Astronomy. Edited by Alan F. M. Moorwood and Iye Masanori. Proceedings of the SPIE, Volume 5492, pp. 1487-1497 (2004).*, A. F. M. Moorwood and M. Iye, eds., pp. 1487–1497, Sept. 2004.
3. J. S. Greaves, W. S. Holland, T. Jenness, A. Chrysostomou, D. S. Berry, A. G. Murray, M. Tamura, E. I. Robson, P. A. R. Ade, R. Nartallo, J. A. Stevens, M. Momose, J.-I. Morino, G. Moriarty-Schieven, F. Gannaway, and C. V. Haynes, "A submillimetre imaging polarimeter at the James Clerk Maxwell Telescope," *MNRAS* **340**, pp. 353–361, Apr. 2003.
4. R. H. Hildebrand, J. A. Davidson, J. L. Dotson, C. D. Dowell, G. Novak, and J. E. Vaillancourt, "A Primer on Far-Infrared Polarimetry," *PASP* **112**, pp. 1215–1235, Sept. 2000.
5. Hecht, E., *Optics*, Addison-Wesley, New York., 1998 (third edition).
6. G. M. Voellmer, D. T. Chuss, M. Jackson, S. H. Moseley, G. Novak, and E. J. Wollack, "A kinematic, flexure-based mechanism for precise, parallel motion for the Hertz Variable-delay Polarization Modulator (VPM)," in *These proceedings*, May 2006.
7. D. A. Schleuning, C. D. Dowell, R. H. Hildebrand, S. R. Platt, and G. Novak, "HERTZ, A Submillimeter Polarimeter," *PASP* **109**, pp. 307–318, Mar. 1997.
8. D. W. Koerner, C. J. Chandler, and A. I. Sargent, "Aperture Synthesis Imaging of the Circumstellar Dust Disk around DO Tauri," *ApJ Lett.* **452**, pp. L69+, Oct. 1995.
9. S. V. W. Beckwith, A. I. Sargent, R. S. Chini, and R. Guesten, "A survey for circumstellar disks around young stellar objects," *AJ* **99**, pp. 924–945, Mar. 1990.

10. J. Rodmann, T. Henning, C. J. Chandler, L. G. Mundy, and D. J. Wilner, "Large dust particles in disks around T Tauri stars," *A&A* **446**, pp. 211–221, Jan. 2006.
11. G. Novak, D. P. Gonatas, R. H. Hildebrand, S. R. Platt, and M. Dragovan, "Polarization of far-infrared radiation from molecular clouds," *ApJ* **345**, pp. 802–810, Oct. 1989.
12. M. Tamura, J. H. Hough, J. S. Greaves, J.-I. Morino, A. Chrysostomou, W. S. Holland, and M. Momose, "First Detection of Submillimeter Polarization from T Tauri Stars," *ApJ* **525**, pp. 832–836, Nov. 1999.
13. R. H. Hildebrand, J. L. Dotson, D. A. Dowell, C. D. Schleuning, and J. E. Vaillancourt, "The Far-Infrared Polarization Spectrum: First Results and Analysis," *ApJ* **516**, pp. 834–842, May 1999.
14. Spitzer, L., *Physics Processes in the Interstellar Medium*, John Wiley and Sons, New York., 1978.